POAC'15
Trondheim, Norway

Proceedings of the 23rd International Conference on
Port and Ocean Engineering under Arctic Conditions
June 14-18, 2015
Trondheim, Norway

SPATIAL SAMPLING SCHEMES FOR SEA ICE DRAFT FROM UPWARD-LOOKING SONAR DATA

Richard McKenna[1], Humfrey Melling[2], Brian Wright[3]

[1] R.F. McKenna Associates, Wakefield, QC, Canada, richard.mckenna@sympatico.ca

[2] Institute of Ocean Sciences, Fisheries and Oceans Canada, Sidney, BC, Canada

[3] B. Wright and Associates Ltd., Canmore, AB, Canada

ABSTRACT

Since 1990, upward-looking sonar data have been collected at various sites in the Canadian Beaufort Sea, providing a unique long-term record of sea ice draft. The draft time series are combined with acoustic Doppler current profiler drift speeds to yield 1m quasi-spatial series for ice drifting over the instrument location. Focus in this paper is on selected data from Site 2, in a water depth of approximately 80m.

For ice management simulations and other analyses, there is incentive to consider not only the two-dimensional spatial series of ice drifting over a point but also a full three-dimensional representation of the ice cover. By assuming that ice draft is isotropic in space, the statistical attributes of the measured drafts and draft increments provide a means of randomly sampling off-track drafts perpendicular to the drift direction. Although some information that could be used to represent linear features such as ridges and leads is intrinsic within the data, this aspect has not been explored here.

This paper provides a brief outline of sampling objectives, a statistical characterization of the data, a comparison of draft and draft increment distributions, a description of spatial sampling schemes, an illustration of sampled fields, and an evaluation of the relative merits of sampling drafts and draft increments. The result is a three-dimensional representation of the ice cover, with off-track values derived from the statistical characteristics of the measured along-track values.

INTRODUCTION

In a previous paper (Wright *et al*, 2014), an ice management simulation procedure was outlined to assess the performance of icebreaking ships for support of a drilling operation in sea ice. A key feature of this effort, first initiated in 2007, was the spatial characterization of the ice cover based on upward-looking sonar data, aerial survey data, and other on-ice field data. Sea ice management potentially involves multiple icebreaking vessels working in complex patterns in a constantly-changing and moving sea ice cover. There are distinct advantages to simulating such procedures in an ice cover that is as realistic as possible and

that provides a complete three-dimensional representation of the ice. One option is to use satellite radar or optical imagery as the basis for representing the ice cover, but ice thickness can only be approximated from such imagery, and drift patterns cannot be resolved on the necessary time scales.

Over 25 years ago, an ice profiling sonar (IPS) was developed at the Institute of Ocean Sciences in Canada. The first comprehensive field report by Melling and Reidel (1993) documented the deployment of these upward-looking sonars (ULS) and their operation in tandem with acoustic Doppler current profilers (ADCP) to provide simultaneous ice thickness profiles and drift velocity measurements. IPS's have been deployed almost continuously at a couple of sites in the Beaufort Sea since 1990, and intermittently at a number of other sites in the Beaufort Sea and elsewhere in the world. There are distinct advantages to using the IPS/ADCP data for ice characterization when conducting ice management simulations; examples are given in McKenna and Wright (2012) and Hamilton *et al* (2011). Disadvantages include the lack of a full three-dimensional picture of the ice, the failure to measure the consolidated layer thickness of ice ridges, and the inability to discriminate multi-year ice at present. The first is addressed in this paper, the second can potentially be estimated based on the thickness of the adjacent ice, and the third is addressed by Fissel *et al* (2014).

In this paper, two sampling methods are developed to use the statistical information contained in the spatial track from ULS data for estimating representative three-dimensional ice thickness fields. The first method involves sampling ice drafts directly, while the second involves draft increments. A small subset of the data from an IPS deployment in the Beaufort Sea in early 2000 has been analysed to assist with the development of these methods.

IPS DATA

The ice-profiling sonar (IPS) is moored in the water column and looks up to the underside of the ice as it drifts by. In this paper, data from Site 2 (70°56.37'N, 133°41.05'W) in the Canadian Beaufort Sea are analysed for a 60-day period from January 1, 2000 to March 1, 2000 (for more details of the deployment, see Melling and Reidel, 2004). Site 2 is located in a water depth of approximately 80m. Ice draft measurements were collected every 4 seconds, with an accuracy of about ±5 cm. An acoustic Doppler current profiler (ADCP) moored nearby measured the speed and direction of ice drift over the instrument averaged over 40 minutes. The ice drift rate and direction change relatively slowly compared with the ice draft, justifying the less frequent ADCP sampling.

A pseudo-spatial transect of under-ice topography was calculated by using the ice-velocity information to map ice draft values at regular intervals of time to points irregularly spaced along the vector of ice displacement. Uniformly spaced ice draft values along the ice displacement were then obtained by interpolation. The result is a spatial series of ice draft points with a constant distance of 1m apart, which is the basis for the analysis performed in this paper.

The pseudo-drift track for January 1, 2000 through March 1, 2000 at Site 2 is shown in Figure 1. Reference is to a pseudo-drift track because it is not the actual trajectory of the ice but a reconstruction of the ice drift trajectory by integrating the ADCP-derived drift velocity as the ice crossed over the instrument. The origin in Figure 1 is based on drift since the integration was initiated on October 1, 1999.

The corresponding spatial series of drafts plotted in 1m increments along the pseudo-drift track is shown in Figure 2. The pseudo-drift track shown in the figure has a length of approximately 230km. The ice drafts in Figure 2 range from 0m, indicating no ice, to a

maximum value of about 15m. Ice draft values are plotted in a positive sense so that Figure 2 represents an inverted view of the undersurface of the ice. All of the ice is first-year, with an initial level-ice thickness of about 0.75m and reaching to nearly 1.5m at the end of the spatial series. There are many ridges in the ice cover and the occasional lead, in which the ice thickness often drops to less than 0.25m. In the lower part of Figure 2, one can see that most of the draft increments are less than 2m and that the larger increments are generally associated with the ridges. Small draft increments are associated either with open water or with continuous expanses of level ice.

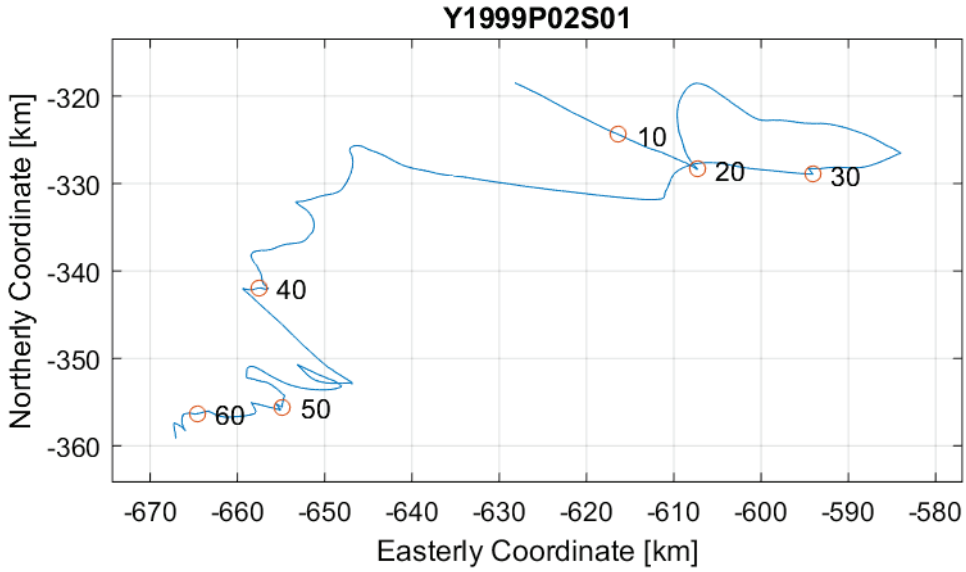

Figure 1 Pseudo-drift track at Site 2 in the Beaufort Sea (70°56.37'N, 133°41.05'W; positions are shown on the track in Julian days for year 2000)

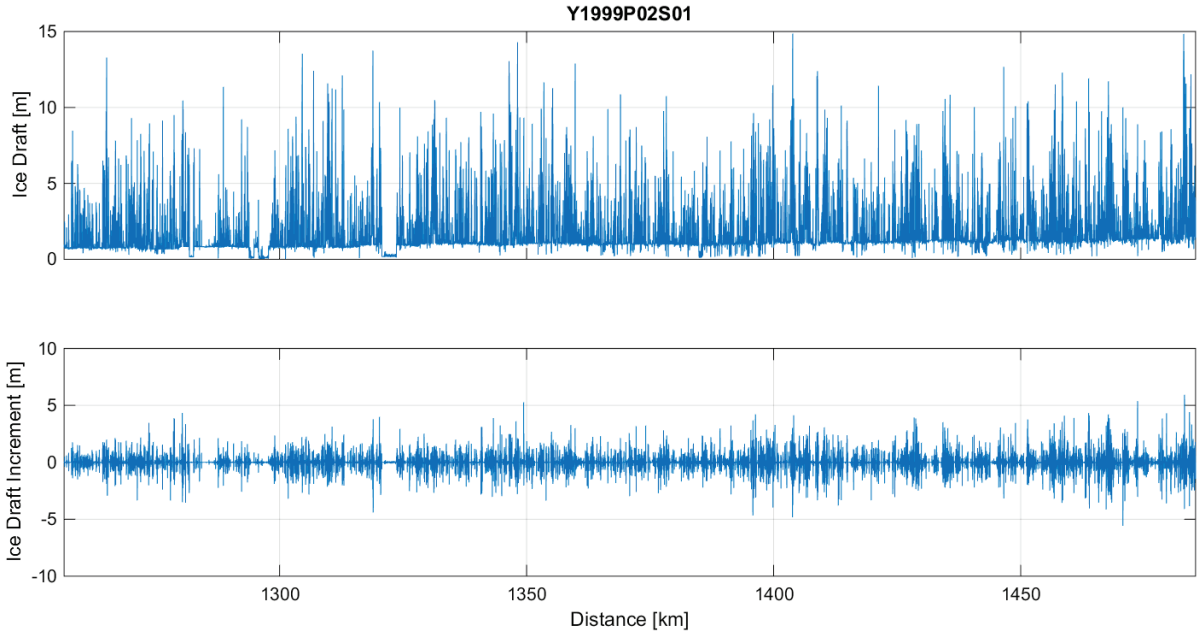

Figure 2 Spatial series plotted on a 1m increment at Site 2 in the Beaufort Sea (70°56.37'N, 133°41.05'W; January 1, 2000 to March 1, 2000; note that distances along the pseudo-drift track start on October 1, 1999)

SPATIAL CORRELATIONS

The ice draft spatial series is $z(x)$, where z is draft and x is distance along the pseudo-drift track. Alternatively, the spatial series can be represented by the sequence, z_i, of draft values spaced 1m apart, where $i = 1$ to m. The p-lag spatial autocorrelation coefficient for the drafts is

$$r_p = \{\sum_{i=1}^{i=m-p}(z_{i+p} - \bar{z})(z_i - \bar{z})\}/[\{\sum_{i=p+1}^{i=m}(z_i - \bar{z})^2\}\{\sum_{i=1}^{i=m-p}(z_i - \bar{z})^2\}]^{1/2} \quad [1]$$

where $\bar{z}$ is the mean value for ice draft. Because the spatial increment is 1m, the lag value, p, and the increment are equivalent and interchangeable. Another way of representing the spatial series is to consider the draft increments

$$\Delta z_i = z_i - z_{i-1} \quad [2]$$

in which z_0 is set equal to z_1 so that Δz_1 is zero. The draft spatial series can be reconstructed from the draft increment series from

$$z_i = z_0 + \sum_{k=1}^{k=i} \Delta z_k \quad [3]$$

where z_0 is the initial draft in the spatial series. The spatial correlations for the draft increments are calculated as for the drafts by replacing z with Δz in Equation [1].

Why consider draft increments rather than drafts? The autocorrelation coefficients are shown for a segment of the Site 2 ULS data for lag distances of up to 50m in Figure 3. While the drafts remain correlated well beyond a distance of 50m, the correlation between increments only persists for a very short distance. While a comprehensive analysis has not been conducted for all of the different ULS sites and data segments, the decay in spatial correlation for draft with separation distance is always very slow, while the decay in the increments is always very rapid. As a consequence, it is potentially easier and more informative to characterize the distribution of draft increments than it is for the distribution of drafts.

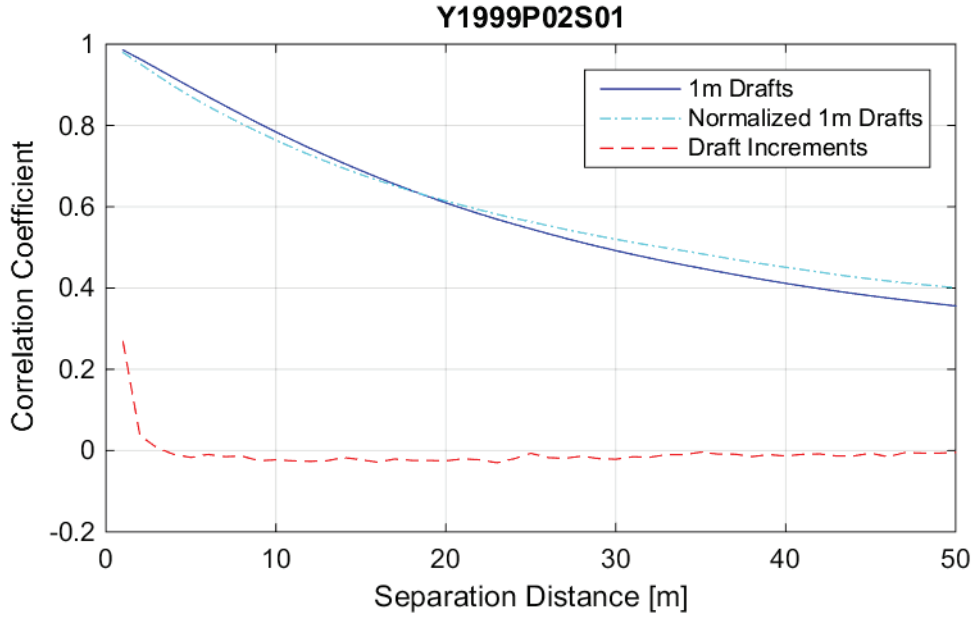

Figure 3 Spatial correlations associated with ice draft and draft increment spatial series at Site 2 (70°56.37'N, 133°41.05'W; January 1, 2000 to March 1, 2000)

In Figure 3, the autocorrelation coefficient is shown for the 1m draft spatial series and for the normalized draft series. The normalized series is obtained by transforming the actual draft distribution to a unit normal distribution. This process is accomplished by sorting the draft data and estimating the cumulative distribution function using a standard plotting position.

Uniformly distributed values are obtained by interpolating the measured drafts through the cumulative distribution function and the unit normal values are obtained by passing the uniform values through the inverse normal distribution function.

SPATIAL SAMPLING

The objective of this paper is to investigate spatial sampling schemes, whereby draft values (z) are sampled in the along-track (x or i) and off-track (y or j) directions, i.e. $z(x,y)$ or $z_{i,j}$. The ULS data are used to initiate the sampling and provide the centreline values in the x or grid i direction, and y or grid j values are sampled on each side of the original track, as shown in Figure 4.

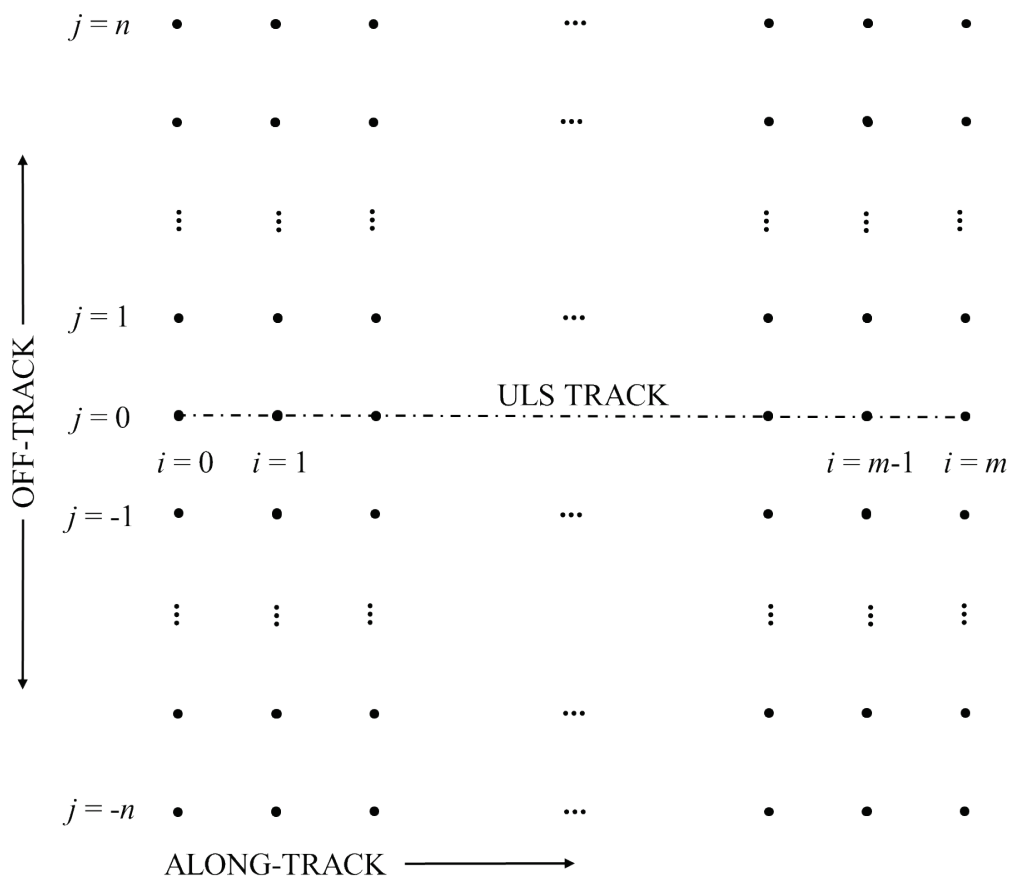

Figure 4 Spatial grid showing original ULS data along centreline and grid positions to be sampled

In the following sections, two different statistical sampling schemes are proposed - the first involves the drafts directly, while the second involves draft increments from which drafts are then calculated. In each case, the objective is to sample values that are representative of the ULS data in a statistical sense. With such sampling schemes, the first issue often raised is whether the process is assumed to be homogeneous; i.e., that the statistical properties are the same from one point in space to the next - in this case, along and off the ULS track. Although statistical homogeneity has been assumed in the following derivations, in that statistical parameters derived from the entire time series segment are used, data could be analysed and applied for any subset of the ULS track that provides accurate enough estimates of the parameters.

A second issue is isotropy - whether the statistical properties are the same regardless of orientation in the plane of the ice surface. A couple of inter-related issues are at stake - the first is whether there is some larger scale process (such as the shear zone of the Beaufort Sea) that influences the properties of the ice, while the second is the orientation of individual ridges or leads. In the present work, isotropic statistical properties for the ice draft have been assumed. Spatial correlations have been estimated along the ULS track and then applied to any other orientation relative to that line. This is important in the context of how ridges are represented. The ULS track crosses many pressure ridges in many different orientations. While the data could be interpreted to ascertain something about ridge orientation, this has not been done in the present work. As a result, the sampling schemes do not capture all of the features of ridges in the Beaufort Sea ice cover. While ridge-like features rising from the surrounding ice are sampled, these do not have the same sinuous or linear shape often found in nature. To capture their shape more fully, more information than can be captured from a single ULS is likely to be required. The same is likely to be the case on a broader scale, and anisotropies over many 100s of metres are not likely to be inferred uniquely from a single ULS.

DRAFT SAMPLING SCHEME

Method

Based on Figure 3, the spatial correlation in ice draft falls off quite slowly. As a result, it is important that the sampling scheme take account of this very important statistical property in the data. A commonly used statistical sampling scheme is the autoregressive model, in which sampled values depend linearly on previously observed or sampled values. Simply stated, the kth value of an autoregressive process with order s is

$$z_k = a_1 z_{k-1} + \cdots + a_s z_{k-s} + e_k \qquad [4]$$

where $a_1 \ldots a_s$ are the weights applied to the values $z_{k-1} \ldots z_{k-s}$ and e_k are random values for which the standard deviation is

$$\sigma_e = \sigma_z \left(1 - \sum r_{01} a_1 + \cdots + r_{0s} a_s\right)^{1/2} \qquad [5]$$

in which σ_z is the standard deviation of the process (ice draft, in this case) and r_{0s} is the spatial autocorrelation coefficient between z_k and z_{k-s}. The weights $a_1 \ldots a_s$ can be calculated by multiplying both sides of Equation [4] by $z_{k-1} \ldots z_{k-s}$, in turn, and taking the expected value to obtain the following system of equations (the Yule-Walker equations)

$$\begin{Bmatrix} r_{01} \\ \vdots \\ r_{0s} \end{Bmatrix} = \begin{bmatrix} r_{11} & \cdots & r_{1s} \\ \vdots & \ddots & \vdots \\ r_{s1} & \cdots & r_{ss} \end{bmatrix} \begin{Bmatrix} a_1 \\ \vdots \\ a_s \end{Bmatrix} = \begin{bmatrix} 1 & \cdots & r_{1s} \\ \vdots & \ddots & \vdots \\ r_{s1} & \cdots & 1 \end{bmatrix} \begin{Bmatrix} a_1 \\ \vdots \\ a_s \end{Bmatrix} \qquad [6]$$

The autocorrelations in the matrix in Equation [6] are the spatial correlation values between the various points on the right hand side of Equation [4]. At the same point in space, i.e. the diagonal elements of the matrix, autocorrelations $r_{11} \ldots r_{ss}$, are unity. As long as the matrix in the system of equations given in Equation [6] is positive definite, a unique set of real weights $a_1 \ldots a_s$ can be calculated.

In the present implementation of the autoregressive model, the data (i.e. the z values in Equation [4]) are converted to a unit normal distribution prior to implementation of the sampling scheme. This simplifies the approach and provides a more robust method because e_k can be sampled from a unit normal distribution that is independent of draft. Use of the normalization also means that $\sigma_z = 1$.

In two dimensions, the idea is basically the same, and the indices k and s in [4] can be replaced by i,j and p,q. How the model is applied depends on the way in which one wants to sample the parameter, $z_{i,j}$, to the grid. In some applications, one might want to fill in one or more values. In the present case, one starts with the known track and one samples values off-track and parallel to the known track. The situation for $p = q = 1$ is shown in Figure 5. The point to be calculated is i,j in the sampling of a new track j that is parallel to the original track or previously calculated track, j-1.

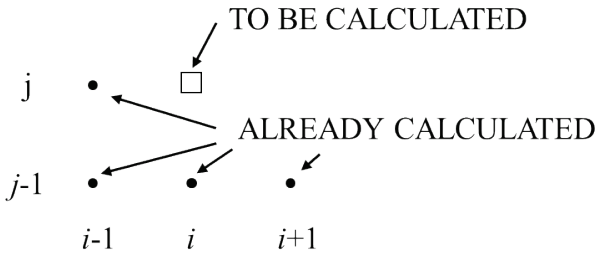

Figure 5 Sampling grid for p=q=1; the i,j point to be sampled is shown by the open square

The situation is not the same at all points in the grid shown in Figure 4. At the start and end of the ULS track and adjacent to it, one obtains cases where $p \neq q$ and where the trailing and leading values of p are different. The general situation is shown in Figure 6, in which p_1 and p_2 are the trailing and leading values, respectively.

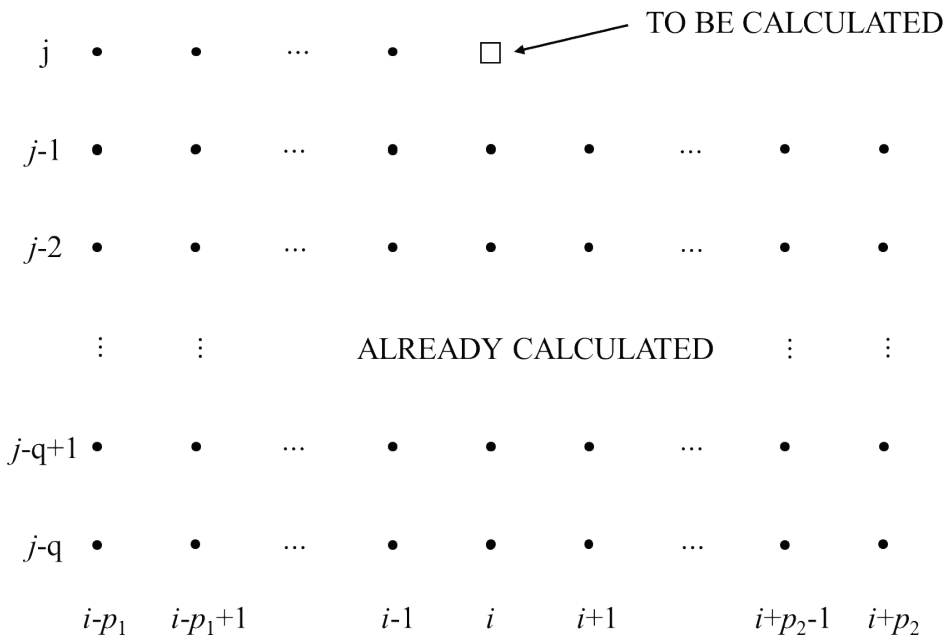

Figure 6 Sampling grid for arbitrary p_1, p_2, q; the i,j point to be sampled is shown by the open square

For an isotropic and homogeneous field $z_{i,j}$, the correlation coefficients in Equation [6] depend only on the distances between the various grid points. As a result, the only parameters involved in the estimation of grid values are those defining the isotropic correlation function. In the present case, the correlation function calculated from the normalized data in Figure 3 is used directly. The other key element of the sampling scheme is the probability distribution of the measured drafts because it is used in the normalization process. As outlined in the spatial

correlation section above, the measured drafts, z, are converted to a unit normal distribution prior to the sampling and then converted back to the original distribution afterwards.

Results

The draft sampling scheme has been applied for illustrative purposes based on the spatial series shown in Figure 2 for Site 2 in the Beaufort Sea (Melling and Reidel, 2004) between January 1, 2000 and March 1, 2000. The mean ice thickness during this period was 1.66m and the standard deviation was 1.46m. When calculating the weights (Equations [4,6]), the spatial autocorrelations were interpolated from the measured values given in Figure 3. The following results are based on $p_1 = p_2 = q = 10$ for most of the grid and less, out of necessity, near the ULS track (in the j direction) and at the start and end of the ULS track (in the i direction). Because the computational effort increases significantly for the calculation of the weights in Equation [6] (i.e. at a rate that depends on $[(p_1 + p_2)\ q]^3$), is not practical to use a region of interest much larger than this in the sampling scheme. Besides, the spatial correlation structure is fairly well captured for this region of interest and larger ones do not improve the correlation structure of the sampled values.

Sampled data for the first 2km of the ULS track are shown in Figure 7. According to the legend, the level ice is shown darker and the ridges are displayed as white, with the deepest ridges about 14m. As in Figure 4, the measured ULS drafts in Figure 7 are along the centreline of the sampled data (and more or less invisible among the surrounding sampled points). In this initial segment of the ULS data, the mean measured draft was 1.10m and the standard deviation was 1.00m. For the sampled grid data in this first 2km segment, the mean value was about 1.3m and the standard deviation was about 1.0m based on repeated sampling efforts. The difference between these statistics, and particularly the mean value, points to a disadvantage of this particular sampling scheme. Although the drafts in this initial portion of the ULS track have a mean of 1.10m (driven by the level-ice thickness of about 0.75m), the sampled values strike a balance between the overall mean for the entire two-month data segment of 1.66m and the mean for this 2km segment of the ULS data. Slight modifications to sampling scheme could account for the trend in the mean as the ice grew over these two months.

In Figure 8, the measured ULS track is shown alongside three other parallel sampled tracks at 125m, 250m, and 375m distances off-track. The sampled data are the same as shown in Figure 7. One feature that is not captured very well by this sampling scheme is clearly evident in Figure 8. While the measured ULS profile shows significant extents of level or near-level ice, the sampled tracks have a slightly more undulating surface. This is probably due to an over estimation in the variability of the ice thickness for small drafts. On the other hand, the shape and characteristics of the ridges appear to be well represented, at least visually.

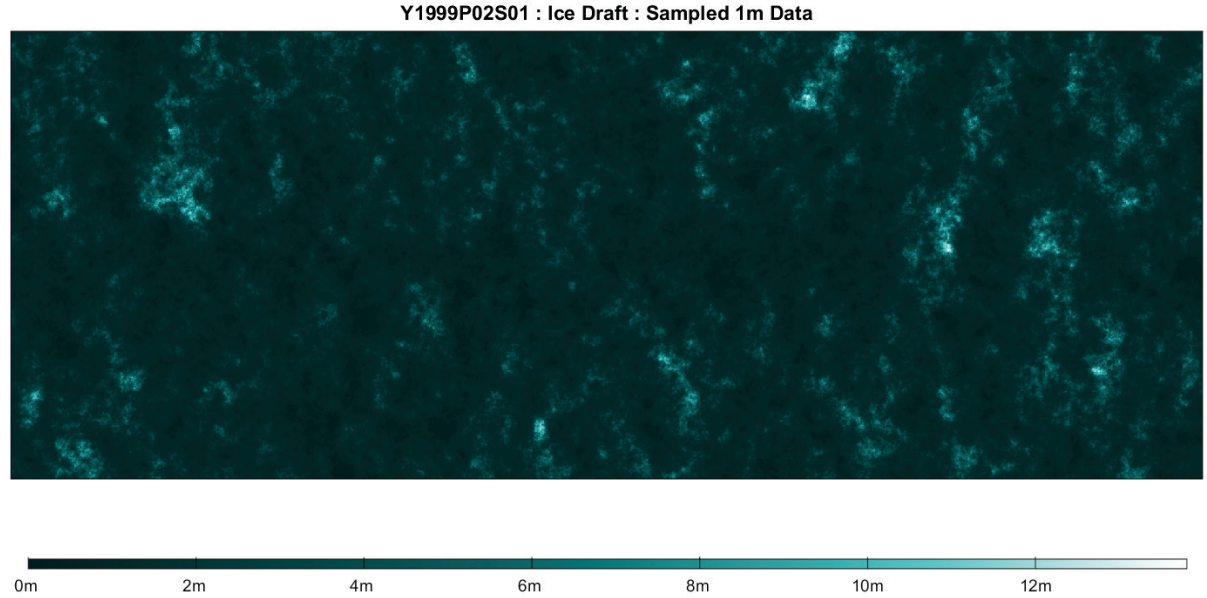

Figure 7 Sampled draft grid values based on draft sampling scheme (2000m along-track, 750m off-track, note also the legend in which thicker ice is white and thinner ice is dark)

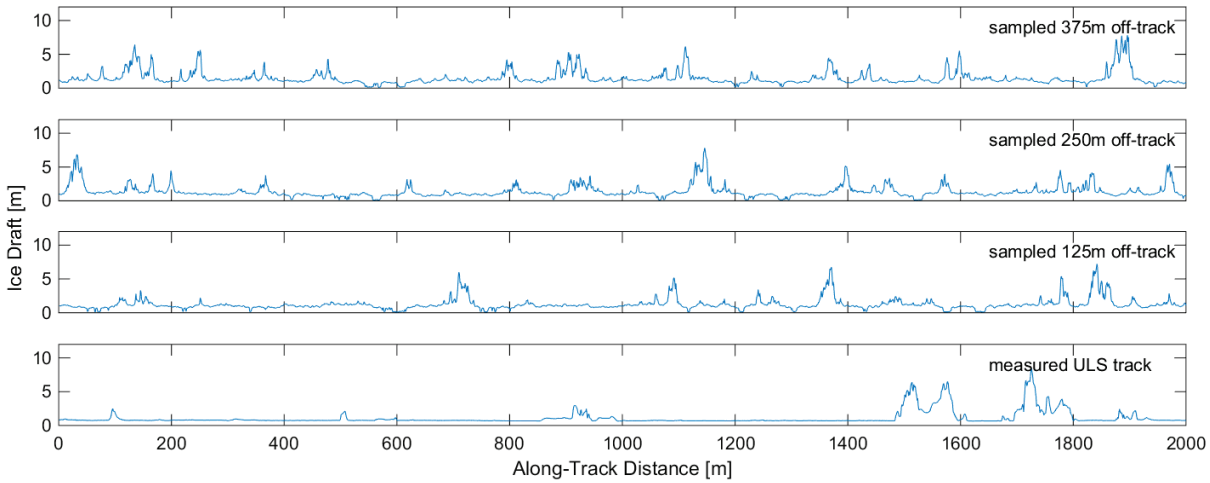

Figure 8 ULS data and sampled draft profiles 125m, 250m, and 375m off-track

DRAFT INCREMENT SAMPLING SCHEME

Draft increment distribution

Recalling Figure 2, the magnitudes of the draft increments appear to depend on the magnitude of the draft. Figure 9 shows cumulative distribution functions of the increments for different draft bins based on the ULS data. To interpret Figure 9, the CDF is the probability that a given draft increment is not exceeded. For example, there is a 0.2 probability of having a draft increment less than -0.5m when the draft is between 10m and 15m. A significant amount of information is contained in the distributions of Figure 9. For the small draft bins, the probability of a positive draft increments is greater than the probability of negative ones. For the middle draft bins, such as the 2m-5m draft range, the probability of positive and negative draft increments is about equal. On the other hand, the probability of sampling negative draft

increments for the larger draft bins, i.e. 5m-10m and 10m-15m, is greater than for sampling positive increments. In other words, increments for small drafts are mostly positive, while increments for larger drafts are mostly negative. Clearly, the distribution of draft increments is quite strongly influenced by the magnitude of the draft and this can be used in the development of a sampling scheme.

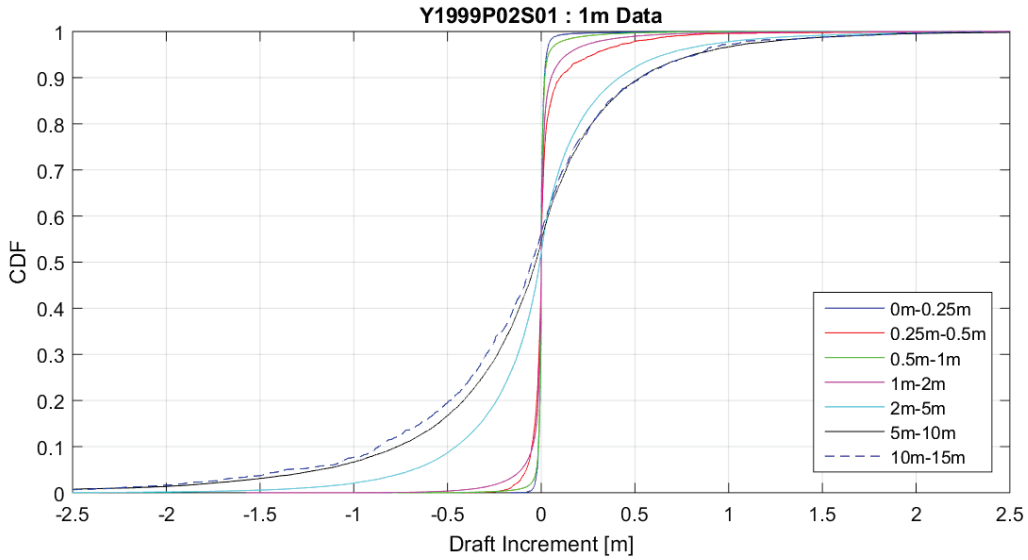

Figure 9 Draft increment distributions for different ice draft bins based on the ULS data in Figure 2

Method using uncorrelated draft increments

Based on Figure 3, there is very little spatial correlation in the draft increments. The first sampling method that was investigated therefore ignored any spatial correlation and assumed uncorrelated increments. Increment distributions of the type shown in Figure 9 were applied to sample off-track increments based initially on the measured track and then successively based on the last sampled value. In other words, off-track profiles in the *j* direction were sampled at each *i* grid point along the track. The resulting statistics were representative of the original data in the off-track direction but adjacent sampled off-track draft values in the profiles diverged with increasing distance off-track. Even though the spatial correlations in the measured draft increments are small, they are obviously significant in the sampling scheme.

Recognizing the importance of spatial correlations in the increments, the next sampling approach that was investigated considered a set of draft increment distributions (like in Figure 9) but based jointly on adjacent draft values on either side of the increment. Although some of the spatial correlation in the measured draft increments is captured in this way, adjacent sampled off-track profiles still tended to diverge with increasing off-track distance.

Relationship between along-track and off-track increments

The spatial correlations in the draft increments (repeated from Figure 3) are shown as red circles in Figure 10. The draft increments along the ULS track (e.g. Equation [2]) represent quantities oriented parallel to the line joining the measurement points. For the grid values sampled using the draft scheme, i.e. Equation [4] and Figure 7, one can calculate correlations in a direction parallel to the measurement points using either the along-track values or the off-

track increments. The black squares in Figure 10 represent the average of these, which were more or less equivalent. The relationships based on the red squares (ULS) and the black squares (draft sampling scheme) are quite similar, indicating that the draft scheme does a reasonable job of representing the increments. An increment sampling scheme needs to also represent off-track values based on along-track values or, conversely, along-track values from off-track values. The black x symbols in Figure 10 are calculated based on correlations between off-track and along-track increments, and labelled as perpendicular values. These are quite different from the parallel correlations, not only for this set of grid values for this dataset but for other datasets sampled using the draft scheme. The difference between the parallel and perpendicular correlations can potentially be exploited in the increment sampling scheme.

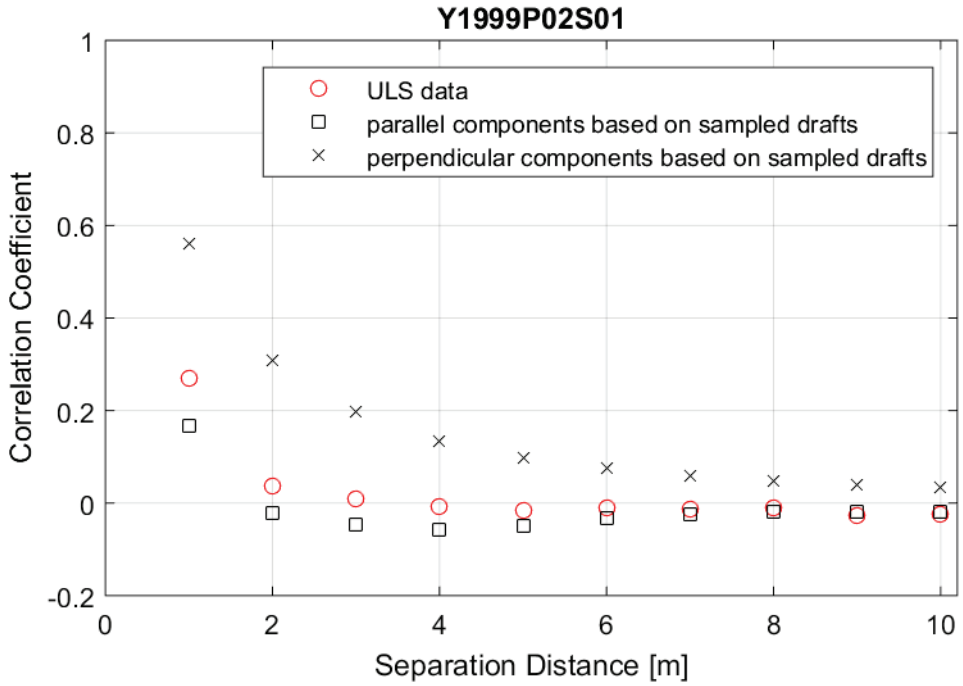

Figure 10 Draft increment correlations: from ULS data, sampled data based on draft scheme

Investigation of method using correlated draft increments

If differences between the along-track and off-track spatial correlations in the draft increments need to be considered, a sampling method similar to the one used for drafts potentially offers an alternative approach. A draft increment sampling scheme can be obtained by replacing z with Δz in Equation [4] and relating the i,j draft increment to the adjacent along-track and off-track increments. The scheme for along-track draft increments is then

$$\Delta z_k = a_1 \Delta z_{k-1} + \cdots + a_s \Delta z_{k-s} + a'_1 \Delta z'_{k-1} + \cdots + a'_s \Delta z'_{k-s} + e_k \qquad [7]$$

where $a_1 \ldots a_s$ are the weights applied to the along-track values $\Delta z_{k-1} \ldots \Delta z_{k-s}$ and $a'_1 \ldots a'_s$ are the weights applied to the off-track values $\Delta z'_{k-1} \ldots \Delta z'_{k-s}$. As in the above Equations [4] through [6], the subscript k is intended to imply i,j. The order of the parameters with k and s subscripts is irrelevant in these equations - the only important thing is that the spatial distance between the various grid points is properly represented when calculating the correlation coefficients.

While increments could be calculated for both along-track and off-track values in the manner of Equation [7], only one set of these needs to be calculated because the *i,j* draft value relates the increments in the following way

$$z_{i,j} = z_{i-1,j} + \Delta z_{i,j} = z'_{i,j-1} + \Delta z'_{i,j} \quad [8]$$

For the draft increment case, there are similar Equations to [5,6] involving along-track and across-track values. The standard deviation is

$$\sigma_e = \sigma_{\Delta z} [1 - \sum(r_{01}a_1 + \cdots + r_{0s}a_s + r'_{01}a'_1 + \cdots + r'_{0s}a'_s)]^{1/2} \quad [9]$$

in which σ_z is the standard deviation of the draft increments, r_{0s} is now the spatial autocorrelation coefficient between Δz_k and Δz_{k-s}, and r'_{0s} is the spatial autocorrelation coefficient between Δz_k and $\Delta z'_{k-s}$. In a similar way to Equation [6], the weights in Equations [7,9] can be calculated using the following system of equations

$$\begin{Bmatrix} r_{01} \\ \vdots \\ r_{0s} \\ r'_{01} \\ \vdots \\ r'_{0s} \end{Bmatrix} = \begin{bmatrix} 1 & \cdots & r_{1s} & r'_{11} & \cdots & r'_{1s} \\ \vdots & \ddots & \vdots & \vdots & \ddots & \vdots \\ r_{s1} & \cdots & 1 & r'_{s1} & \cdots & r'_{ss} \\ r'_{11} & \cdots & r'_{1s} & 1 & \cdots & r''_{1s} \\ \vdots & \ddots & \vdots & \vdots & \ddots & \vdots \\ r'_{s1} & \cdots & r'_{ss} & r''_{s1} & \cdots & 1 \end{bmatrix} \begin{Bmatrix} a_1 \\ \vdots \\ a_s \\ a'_1 \\ \vdots \\ a'_s \end{Bmatrix} \quad [10]$$

In the above, the correlations r''_{1s}, etc, relating the off-track increments associated with different grid points are equivalent to the along-track correlations r_{1s}. The off-diagonal sub-matrices are equal because it does not matter which end of a line one relates an along-track increment and an off-track one on account of isotropy.

Preliminary investigations have been made with a draft increment sampling scheme based on Equations [8,9,10] and the approach shows some promise in representing the statistics of the measured ULS draft data. One of the challenges with this approach is the estimation of correlations for increment components perpendicular to the direction of measured values. This can either be done theoretically or based on datasets where drafts have been measured using multiple ULS units or multibeam sonar imaging systems.

CONCLUSIONS AND RECOMMENDATIONS

A sampling procedure for sea ice draft has been developed that successfully encapsulates the statistical characteristics of two-dimensional ULS/ADCP ice draft profiles along pseudo-tracks and produces statistically representative three-dimensional fields. While this is a significant result, the sampling procedure cannot fully characterize the plan shape of ice ridges due to the assumption of isotropy in the drafts.

The development of a sampling method based on draft increments has proved to be more complex than anticipated since schemes involving uncorrelated increments cannot replicate the statistical attributes of the measured profile data. Work is ongoing to develop a simple and efficient approach to adequately represent along-track and off-track increments.

Although regional and seasonal effects are not addressed in the paper, the statistical parameters relating to ice draft vary from place to place, from season to season (e.g. Melling and Reidel, 1996), and from year to year. There would be considerable merit in quantifying ice draft statistically, using a small number of parameters, and to use them as a basis for

comparison of ice cover characteristics. The present sampling approaches are well suited for addressing regional and seasonal effects.

Total ice draft is but one of the parameters that can influence the performance of icebreaking vessels. Information on the presence of multi-year ice, floe dimensions, and ridge consolidation can potentially be inferred from ULS/ADCP data as well. The approach outlined in the paper provides a basis for the assimilation of these types of data into spatial sampling schemes.

Continued efforts are underway using data from ULS/ADCP deployments in the Beaufort Sea and elsewhere to assess the effectiveness of ice management strategies.

REFERENCES

Fissel, D.B., Ross, E., Sadova, L., Slonimer, A., Sadowy, D. and Mudge, T.D. 2014. The Detection of Multi-Year Ice Using Upward Looking Sonar Data, in Proceedings of the 11th International Conference and Exhibition on Performance of Ships and Structures in Ice, Paper ICETECH14-158-RF, Banff, AB, Canada, July 28-31, 2014.

Hamilton, J., Holub, C., Blunt, J., Mitchell, D. and Kokkinis, T. 2011. Ice Management for Support of Arctic Floating Operations, OTC Paper 22105, presented at the Arctic Technology Conference, Houston, Texas, USA.

McKenna, R. and Wright, B. 2012. Assessment of Ice Management Success in Pack Ice, in Proceedings of the ICETECH 2012 International Conference and Exhibition on Performance of Ships and Structures in Ice, Paper No. ICETECH12-151-R1, Banff, AB, Canada, 17-20 September 2012.

Melling, H. and Riedel, D.A. 1993. Draft and Movement of Pack Ice in the Beaufort Sea, Canadian Technical Report of Hydrography and Ocean Sciences 151, Fisheries and Oceans Canada, 79p.

Melling, H. and Riedel, D.A. 1996. Development of Seasonal Pack Ice in the Beaufort Sea during the Winter of 1991-1992: A View from Below. Journal of Geophysical Research: Oceans, Volume 101, Issue C5, pages 11975–11991.

Melling, H. and Riedel, D. A. 2004. Draft and Movement of Pack Ice in the Beaufort Sea: A Time-Series Presentation April 1990 – August 1999, Canadian Technical Report of Hydrography and Ocean Sciences 238, Fisheries and Oceans Canada, 24p.

Wright, B., McKenna, R., and Browne, R. 2014. A Tactical Ice Management Simulation Methodology and Approach, in Proceedings of the 2014 Arctic Technology Conference, Paper ATC 1748342, Houston, TX, USA, 10-12 February 2014.